ChemPubSoc Europe

DOI: 10.1002/open.201700028

Open Access ChemistryOPEN Full Papers

Nature of the Ru–NO Coordination Bond: Kohn–Sham Molecular Orbital and Energy Decomposition Analysis

Renato P. Orenha,[a, b] Marcus V. J. Rocha,[b, c] Jordi Poater,*[d, e] Sérgio E. Galembeck,*[a] and F. Matthias Bickelhaupt*[b, f]

We have analyzed structure, stability, and Ru–NO bonding of the *trans*-$[RuCl(NO)(NH_3)_4]^{2+}$ complex by using relativistic density functional theory. First, we focus on the bond dissociation energies associated with the three canonical dissociation modes leading to $[RuCl(NH_3)_4]^+ + NO^+$, $[RuCl(NH_3)_4]^{2+} + NO$, and $[RuCl(NH_3)_4]^{3+} + NO^-$. The main objective is to understand the Ru–NO^+ bonding mechanism in the conceptual framework of Kohn–Sham molecular orbital theory in combination with a quantitative energy decomposition analysis. In our analyses, we have addressed the importance of the synergism between Ru–NO^+ σ-donation and π-backdonation as well as the so-called negative *trans* influence of the Cl^- ligand on the Ru–NO bond. For completeness, the Ru–NO^+ bonding mechanism is compared with that of the corresponding Ru–CO bond.

1. Introduction

Nitric oxide (NO) is involved in a large number of physiological and physiopathological processes, such as a biological messenger responsible for vasodilation, playing an important role in immune response, or acting as a neurotransmitter.[1] Thus, owing to the importance of NO, which can either be beneficial or harmful depending on its concentration and bioavailability,[1f] studies concerning NO donors and scavengers have experienced large growth.[2] Major advances in this area have been achieved with ruthenium tetraammine nitrosyl complexes *trans*-$[Ru^{II}(NO^+)(NH_3)_4L]^{n+}$, which appear to have a low cytotoxicity towards host cells, are water soluble, and stable against air oxidation. In such complexes, the role of the *trans* ligand L is crucial, because it modulates the reactivity of the *trans* ligand NO^+.[2h] An example is the negative *trans* influence, that is, the bond strengthening effect, of $L = Cl^-$ on the Ru–NO^+ bond in *trans*-$[Ru^{II}(NO^+)(NH_3)_4Cl]^{2+}$,[3] shown below:

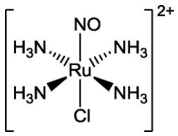

In this context, the Ru–NO chemical bond can be described in terms of the $\{RuNO\}^n$ notation, where *n* holds for the sum of the number of electrons in 4d orbitals of Ru, and π* orbital of NO, as proposed by Enemark and Feltham.[3b] The importance of this definition is based on the fact that NO is referred to as a "non-innocent" ligand, that is, the oxidation state of this ligand cannot be defined in a clear way in these metal complexes.[3c] Another point is that this bond between ruthenium and the π acceptor ligand nitrosyl can be expected to have a synergism between two processes: σ-donation from NO to d_σ of Ru, plus π-backdonation from d_π orbital of Ru to π* of NO.[3a]

The purpose of the present study is twofold. In the first place, we have analyzed the electronic structure and energetically preferred dissociation modes in order to determine the effective oxidation state and most suitable canonical form of the NO ligand in the complex. Thus, we have carried out an investigation based on three possible dissociation reactions for

[a] R. P. Orenha, Prof. Dr. S. E. Galembeck
Departamento de Química, Faculdade de Filosofia
Ciências e Letras de Ribeirão Preto, USP
Ribeirão Preto-SP, 14040-901 (Brazil)
E-mail: segalemb@usp.br

[b] R. P. Orenha, Dr. M. V. J. Rocha, Prof. Dr. F. M. Bickelhaupt
Department of Theoretical Chemistry and
Amsterdam Center for Multiscale Modeling (ACMM)
Vrije Universiteit Amsterdam
De Boelelaan 1083, 1081 HV Amsterdam (The Netherlands)

[c] Dr. M. V. J. Rocha
Fluminense Federal University
Institute of Chemistry—Department of Physical Chemistry
Outeiro de São João Baptista, 24020-141 Niteroi, Rio de Janeiro (Brazil)

[d] Prof. Dr. J. Poater
ICREA, Pg. Lluís Companys 23
08010 Barcelona (Spain)

[e] Prof. Dr. J. Poater
Departament de Química Inorgànica i Orgànica & IQTCUB
Universitat de Barcelona
08028 Barcelona, Catalonia (Spain)

[f] Prof. Dr. F. M. Bickelhaupt
Institute for Molecules and Materials
Radboud University
Heyendaalseweg 135, 6525 AJ Nijmegen (The Netherlands)
E-mail: F.M.Bickelhaupt@vu.nl

Supporting Information and the ORCID identification number(s) for the author(s) of this article can be found under: http://dx.doi.org/10.1002/open.201700028.

the *trans*-$[RuCl(NO)(NH_3)_4]^{2+}$ complex to give either 1) $[RuCl(NH_3)_4]^{+} + NO^{+}$, 2) $[RuCl(NH_3)_4]^{2+} + NO$, or 3) $[RuCl(NH_3)_4]^{3+} + NO^{-}$.

Next, we aim to shed light on the bonding mechanism of the Cl–Ru–NO unit in this complex through detailed quantitative Kohn–Sham molecular orbital and energy decomposition analyses. Here, we anticipate an important role of the synergism between σ-donation and π-backdonation between Ru and NO. Furthermore, we elucidate the mechanism behind the negative *trans* influence of Cl^{-} on the Ru–NO coordination bond. Finally, we compare the nature of the Ru–NO bond with that of Ru–CO in the isoelectronic *trans*-$[RuCl(CO)(NH_3)_4]^{+}$ complex.

Theoretical Methods

Computational Details

All calculations were performed with the Amsterdam Density Functional (ADF) software developed by Baerends and co-workers.[4,5] Molecular orbitals (MOs) were expanded by using one large, uncontracted set of Slater-type orbitals (STO): TZ2P for geometry optimization, vibrational analysis, and single-point energy calculations.[6] The TZ2P basis set is of triple-ζ quality, augmented by two sets of polarization functions (d and f on heavy atoms; 2p and 3d sets on H). All electrons are included in the variational treatment (no frozen-core approximation used). An auxiliary set of s, p, d, f, and g Slater-type orbitals was used to fit the molecular density and to represent the Coulomb and exchange potentials accurately in each self-consistent field (SCF) cycle.[7]

Energies and gradients were calculated by using the local density approximation (LDA: Slater[8] exchange and VWN[9] correlation) with gradient corrections,[10,11] owing to Becke (exchange) and Perdew (correlation) added self-consistently. This is the BP86 density functional. Scalar relativistic corrections were included self-consistently using the zeroth order regular approximation (ZORA).[12] All open-shell systems were treated with the spin-unrestricted formalism. Vibrational analyses for all optimized geometries demonstrate that they are all energy minima at the level of theory applied here.

Energy Decomposition Analysis

All bonding analyses have been carried out at the ZORA-BP86/TZ2P level of theory. The overall bond energy ΔE between $[RuCl(NH_3)_4]^{+2-q}$ and NO^{q} ($q = +1, 0, -1$) is made up of two major components [Eq. (1)]:[13]

$$\Delta E = \Delta E_{strain} + \Delta E_{int} \quad (1)$$

Here, the strain energy ΔE_{strain} is the amount of energy required to deform the fragments NO^{q}, and $[RuCl(NH_3)_4]^{+2-q}$, from their equilibrium structure to the geometry that they acquire in the overall *trans*-$[RuCl(NO)(NH_3)_4]^{2+}$ complex. The interaction energy ΔE_{int} corresponds to the actual energy change when, for example, the geometrically deformed $[RuCl(NH_3)_4]^{+}$ and NO^{+} are combined to form the overall complex.

Later on in our analysis, we focus on the interaction energy ΔE_{int}. The latter can be further analyzed, in the framework of the Kohn–Sham molecular orbital (MO) model, using an energy decomposition analysis (EDA) into electrostatic interaction attraction, Pauli repulsion, and (attractive) orbital interactions [Eq. (2)]:[4,13]

$$\Delta E_{int} = \Delta V_{elstat} + \Delta E_{Pauli} + \Delta E_{oi} \quad (2)$$

The term ΔV_{elstat} corresponds to the classical electrostatic interaction between the unperturbed charge distributions of the prepared (i.e. deformed) $[RuCl(NH_3)_4]^{+}$, and NO^{+}. This term is usually attractive. The Pauli-repulsion ΔE_{Pauli} comprises the destabilizing interactions between occupied orbitals and is responsible for the steric repulsion. The orbital interaction ΔE_{oi} in any MO model, and therefore also in Kohn–Sham theory, accounts for charge transfer (i.e., donor-acceptor interactions between occupied orbitals on one moiety with unoccupied orbitals of the other, including the HOMO–LUMO interactions) and polarization (empty/occupied orbital mixing on one fragment due to the presence of another fragment). The orbital interaction energy can also be decomposed into the contributions from each irreducible representation Γ of the interacting system [Eq. (3)]:

$$\Delta E_{oi} = \Sigma_{\Gamma} \Delta E_{\Gamma} \quad (3)$$

Then, concerning the three possible dissociation reactions for *trans*-$[RuCl(NO)(NH_3)_4]^{2+}$, we must take into account that $[RuCl(NH_3)_4]^{2+}$ and NO fragments [dissociation (2)] have one unpaired electron, whereas $[RuCl(NH_3)_4]^{3+}$ and NO^{-} [dissociation (3)] have two unpaired electrons each. The unpaired electrons in Ru fragments are located in d_{π} fragment molecular orbitals (FMOs), and for NO and NO^{-} are located in π* FMOs (see also Figure 1).

Analysis of the Charge Distribution

The electron density distribution is analyzed at ZORA-BP86/TZ2P by using the Voronoi Deformation Density (VDD) method[14,15] for computing atomic charges. The VDD atomic charge Q_A^{VDD} is computed as the (numerical) integral[16] of the deformation density $\Delta\rho(\mathbf{r}) = \rho(\mathbf{r}) - \Sigma_B \rho_B(\mathbf{r})$ in the volume of the Voronoi cell of atom A [Eq. (4)]. The Voronoi cell of atom A is defined as the compartment of space bound by the bond midplanes on and perpendicular to all bond axes between nucleus A and its neighboring nuclei (cf. the Wigner–Seitz cells in crystals).[15b]

$$Q_A^{VDD} = -\int_{\substack{\text{Voronoi}\\ \text{cell atom A}}} \left[\rho(\mathbf{r}) - \sum_B \rho_B(\mathbf{r})\right] d\mathbf{r} \quad (4)$$

In Equation (4), $\rho(\mathbf{r})$ is the electron density of the molecule and $\Sigma_B \rho_B(\mathbf{r})$ the superposition of atomic densities ρ_B of a fictitious promolecule without chemical interactions that is associated with the situation in which all atoms are neutral. The interpretation of the VDD charge Q_A^{VDD} is rather straightforward and transparent. Instead of measuring the amount of charge associated with a particular atom A, Q_A^{VDD} directly monitors how much charge flows, owing to chemical interactions, out of ($Q_A^{VDD} > 0$) or into ($Q_A^{VDD} < 0$) the Voronoi cell of atom A, that is, the region of space that is closer to nucleus A than to any other nucleus.

In addition, it is also possible to compute the charge rearrangement ΔQ_A^{VDD} with respect to an initial density that is the sum of polyatomic subsystems ρ_i instead of the sum of monoatomic densities [Eq. (5)]:

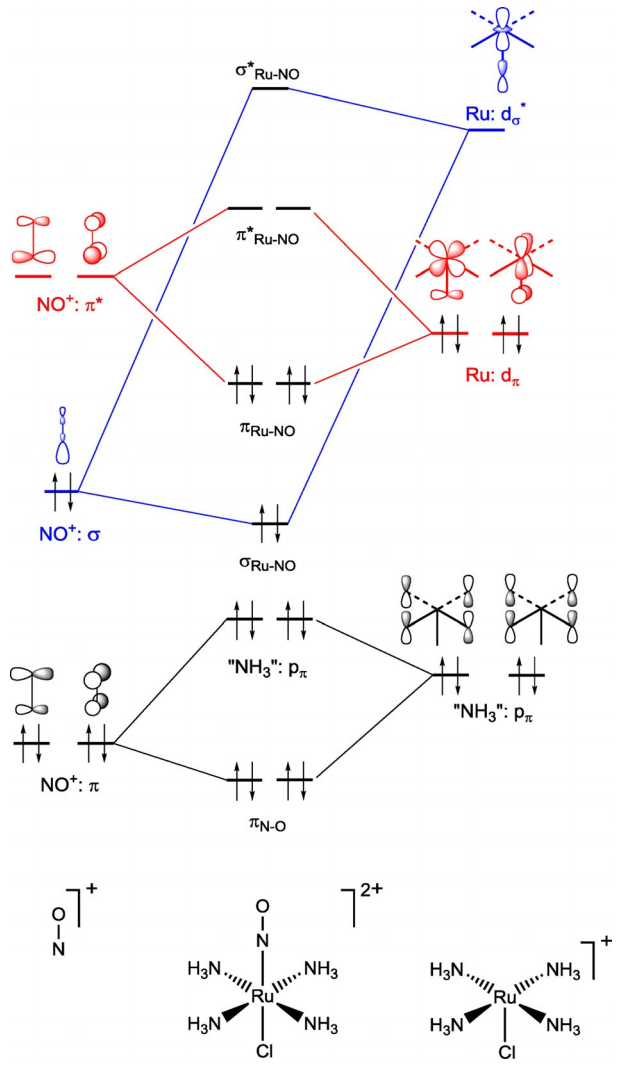

Figure 1. Orbital interaction diagram with the processes of σ-donation (blue) and π-backdonation (red) for *trans*-$[RuCl(NO)(NH_3)_4]^{2+}$ composed of NO^+ and $[RuCl(NH_3)_4]^+$, emerging from our Kohn–Sham orbital analyses at ZORA-BP86/TZ2P.

$$\Delta Q_A^{VDD} = -\int_{\text{Voronoi cell of A in molecule}} \left[\rho(\mathbf{r}) - \sum_{\text{subsystems}} \rho_i(\mathbf{r})\right] d\mathbf{r} \quad (5)$$

Equation (5) offers direct insight into the redistribution of the electronic density caused by the formation of a bond between polyatomic subsystems.[4] This last scheme will be used in the next section to analyze the electron-density distribution of the isolated and deformed fragments that form the complex.

2. Results and Discussion

2.1. Accuracy and Relativistic Effects

Our computed ZORA-BP86/TZ2P and BP86/TZ2P geometrical data and bond-dissociation energies ΔE for the three dissociation schemes are summarized in Table 1, where we compare our calculated results, with and without ZORA relativistic correction, to the experimental values obtained from X-ray diffraction.[17] As can be seen, the computed geometries are in good agreement with the experimental ones. The slightly smaller deviation when ZORA is included demonstrates the significance of relativistic effects and justifies the effort of using the relativistic formalism ZORA-BP86/TZ2P in all further analyses in this study.

Table 1. Geometric data and bond dissociation energies ($-\Delta E$) for *trans*-$[RuCl(NO)(NH_3)_4]^{2+}$ complex.[a]

	ZORA	NR	EXP[b]
Bond distances [Å]			
Ru–NO	1.838	1.825	1.799
N–O	1.150	1.147	1.026[c]
Ru–Cl	2.238	2.278	2.376
Ru–NH_3	2.159	2.175	2.100[d]
Bond angles [°]			
Ru–N–O	180.0	180.0	176.6
Cl–Ru–NO	180.0	180.0	177.9
NH_3–Ru–NO	92.5	93.4	92.0[d]
NH_3–Ru–Cl	87.5	86.6	88.1[d]
NH_3–Ru–NH_3	89.9	89.8	90.0[d]
$-\Delta E$ **[kcal mol^{-1}]**			
$[RuCl(NH_3)_4]^+ + NO^+$	56.6	48.3	[e]
$[RuCl(NH_3)^4]^{2+} + NO$	84.6	79.5	[e]
$[RuCl(NH_3)_4]^{3+} + NO^-$	467.2	465.3	[e]

[a] Computed at BP86/TZ2P with relativistic effects (ZORA), without relativistic effects (NR), and experimental values (EXP). [b] Experimental values from Ref. [17a]. [c] Not reliable due to disorder problems, as mentioned in Ref. [17c]. [d] Average value of the experimental results from Ref. [17a]. [e] Not available.

2.2. Structure and Stability

We first focused on choosing the most suitable canonical form for *trans*-$[RuCl(NO)(NH_3)_4]^{2+}$ complex based on two criteria: the energetically preferred dissociation mode and the geometry. To this end, Table 1 contains the bond dissociation energy (ΔE) for the three above proposed decomposition schemes. The first dissociation of *trans*-$[RuCl(NO)(NH_3)_4]^{2+}$ in $[RuCl(NH_3)_4]^+ + NO^+$ shows the lowest energetic value (56.6 kcal mol^{-1}), as compared to the other two dissociation patterns (82.8 and 466.7 kcal mol^{-1}, respectively). This is a direct consequence of a more favorable Coulomb energy as the two-fold positive charge is separated over two singly positively charged fragments. Thus, *trans*-$[RuCl(NO)(NH_3)_4]^{2+}$ dissociates preferentially into $[RuCl(NH_3)_4]^+ + NO^+$, the latter fragment being isoelectronic with the CO ligand.

Furthermore, the *trans*-$[RuCl(NO)(NH_3)_4]^{2+}$ compound assumes the geometry of a distorted octahedron with C_{4v} symmetry. As shown in Table 1, the NH_3–Ru–NO (92.5°), and NH_3–Ru–Cl (87.5°) angles deviate from 90°; and with Ru–NO, Ru–Cl, and Ru–NH_3 bond lengths of 1.838, 2.238, and 2.159 Å, respectively. However, the most relevant data include the Ru–N–O bond angle of 180°, which has been previously attributed to *trans*-$[Ru(NH_3)_4(Cl)(NO)]^{2+}$, having predominantly $[RuCl(NH_3)_4]^+ + NO^+$ character, based on the fact that the overall complex is EPR silent.[2h,3d] In addition, the reactions of these nitrosyl com-

plexes with hydroxide ions, yielding *trans*-$[Ru(NH_3)_4(L)(NO_2)]^+$, also confirm the nitrosonium character of the [NO] ligand.[17b] Further details of the optimized geometries are provided in the Supporting Information.

Our analyses show that the nature of *trans*-$[RuCl(NO)(NH_3)_4]^{2+}$ is best represented by the $[Ru^{II}\text{-}NO^+]$ canonical form. Therefore, we will cast our further analyses and discussion of the Ru–NO bonding mechanism in terms of the $[RuCl(NH_3)_4]^+ + NO^+$ fragments.

2.3. Ru–NO Bonding Mechanism in *trans*-$[RuCl(NO)(NH_3)_4]^{2+}$

The Ru–NO bonding analysis comprises a quantitative Kohn–Sham molecular orbital analysis complemented with an energy decomposition analysis on *trans*-$[RuCl(NO)(NH_3)_4]^{2+}$ formed from $[RuCl(NH_3)_4]^+$ and NO^+ fragments (I). This EDA is later complemented by two more EDA schemes: II) $[Ru(NH_3)_4]^{2+}$ and NO^+, to analyze the Ru–NO bond in absence of Cl^-; and III) $[Ru(NH_3)_4]^{2+}$ and Cl^-, to investigate Ru–Cl in the absence of NO^+. The combination of the three should give us a complete picture of the Ru–NO interaction in our *trans*-$[RuCl(NO)(NH_3)_4]^{2+}$ complex, with emphasis on the synergy between σ-donation and π-backdonation in the Ru–NO interaction, and also on the negative *trans* influence of the Cl^- ligand.

We first focus on the decomposition scheme that we proposed for our *trans*-$[RuCl(NO)(NH_3)_4]^{2+}$ complex, that is, $[RuCl(NH_3)_4]^+$ and NO^+ (Table 2). The bonding interaction is attractive (−64.6 kcal mol^{-1}). Interestingly, this is exclusively attributed to the orbital interactions ΔE_{oi} (−234.7 kcal mol^{-1}). The latter compensate both the electrostatic term ΔV_{elstat} (55.2 kcal mol^{-1}), which is repulsive because of Coulomb repulsion between the two singly positively charged fragments that are formed, and the repulsive Pauli interaction (115.0 kcal mol^{-1}).

The ΔE_{oi} term (Figure 1) can be further decomposed into σ and π contributions, which amount to −32.5 and −196.3 kcal mol^{-1}, respectively. Note that the π orbital term is by far the dominant contributor of stabilization in the Ru–NO bond. From the gross Mulliken populations of the fragment molecular orbitals (FMOs), we observe σ-donation from NO^+:σ ($P = 1.71$ e) to $Ru:d_\sigma^*$ ($P = 0.32$ e) and π-backdonation from $Ru:d_\pi$ ($P = 1.43$ e) to NO^+:π* ($P = 0.56$ e). The origin of the stronger π-backdonation is the smaller energy difference between the interacting π FMOs compared to the σ ones (7.7 vs. 16.7 eV, respectively). The corresponding FMO overlaps support both σ-donation and π-backdonation interactions; the former being larger (0.38) compared to the latter (0.14). Finally, according to the VDD charge analysis, such larger π-backdonation also translates into a net transfer of 0.892 e to the NO^+ ligand (see Table 2).

Next, we studied the synergism between the σ-donation and the π-backdonation processes present between $[RuCl(NH_3)_4]^+$ and NO^+ fragments. Thus, if we want to only focus on the σ-donation, we have to remove π virtual orbitals of NO^+. On the other hand, if we are interested in π-backdonation, σ virtual orbitals of Ru fragment must be deleted. Note that this deletion of virtuals on one fragment also suppresses polarization between the occupied and virtual orbitals within the same fragment.

Table 2. Analysis of Ru–L^1 bond between $[RuL^2(NH_3)_4]^{n+}$ and L^1 in *trans*-$[Ru(L^1)(L^2)NH_3)_4]^{n+}$ complex.[a]

	I	II	III	
L^1	NO^+	NO^+	Cl^-	CO
L^2	Cl^-	–	–	Cl^-
n	1	2	2	1
EDA [kcal mol^{-1}]				
ΔV_{elstat}	55.2	171.7	−304.7	−136.8
ΔE_{Pauli}	115.0	79.3	139.6	192.4
ΔE_σ	−32.5	−43.0	−67.3	−52.1
ΔE_π	−196.3	−151.9	−21.3	−72.6
$\Delta E_{A2,B1,B2}$	−5.9	−4.9	−3.7	−0.1
ΔE_{oi}	−234.7	−199.8	−92.3	−124.8
ΔE_{int}	−64.6	51.2	−257.5	−69.2
FMO energy [eV]				
$Ru:d_\sigma^*$	−6.5	−14.2	−14.2	−6.9
$Ru:d_\pi$	−7.9	−14.3	−14.3	−8.1
$Cl^-:p_\sigma$	–	–	0.6	–
$Cl^-:p_\pi$	–	–	0.6	–
$L^1:\sigma$	−23.2	−23.2	–	−9.2
$L^1:\pi^*$	−15.6	−15.6	–	−2.4
FMO overlap, *S*				
$<Cl^-:p_\sigma \mid Ru:d_\sigma^*>$	–	–	0.25	–
$<Cl^-:p_\pi \mid Ru:d_\pi>$	–	–	0.11	–
$<L^1:\sigma \mid Ru:d_\sigma^*>$	0.38	0.30	–	0.47
$<Ru:d_\pi \mid L^1:\pi^*>$	0.14	0.13	–	0.22
$<Ru:d_\pi \mid L^1:\pi>$	0.09	0.08	–	0.10
FMO populations, *P* [e]				
$Ru:d_\sigma^*$	0.32	0.37	0.53	0.56
$Ru:d_\pi$	1.43	1.53	1.97	1.73
$Cl^-:p_\sigma$	–	–	1.43	–
$Cl^-:p_\pi$	–	–	1.92	–
$L^1:\sigma$	1.71	1.64	–	1.48
$L^1:\pi$	1.99	1.99	–	1.99
$L^1:\pi^*$	0.56	0.47	–	0.27
VDD charge rearrangement	**ΔQ [a.u.]**[b]			
$[RuL^2(NH_3)_4]^{n+}$	+0.892	+0.712	−0.226	+0.320

[a] Computed at ZORA-BP86/TZ2P. [b] Based on Equation (5).

Table 3. Analysis of the synergy between σ-donation and π-backdonation orbital interactions in $[RuCl(NH_3)_4]^+ + NO^+$ [kcal mol^{-1}].[a]

OI allowed[b]	ΔE_σ	ΔE_π	$\Delta E_{A2,B1,B2}$	ΔE_{oi}	ΔE_{int}
σ-don. + π-back.	−32.5	−196.3	−5.9	−234.7	−64.6
σ-don.	−30.6	0.0	−5.6	−36.2	133.9
π-back.	0.0	−168.2	−6.8	−175.0	−4.8

[a] Computed at ZORA-BP86/TZ2P level. [b] OI = orbital interactions; σ-don. = σ-donation; π-back. = π-backdonation.

When π-backdonation is turned off (see Table 3), ΔE_σ is only slightly reduced, by 1.9 kcal mol^{-1}. On the other hand, when σ-donation is turned off, ΔE_π experiences a considerable weakening by 28.1 kcal mol^{-1}. This reduction in ΔE_π is also observed in the gross Mulliken populations, which show a smaller π charge transfer ($Ru:d_\pi = 1.55$ and $NO^+:\pi^* = 0.44$). Therefore, the synergy effect amounts to $\Delta E_{synergy} = \Delta E_{oi}$(σ-donation + π-backdonation) − ΔE_{oi}(σ-donation only) − ΔE_{oi}(π-backdonation only) =

-23.5 kcal mol^{-1}. Furthermore, concerning the overall charge transfer between the two fragments, when σ-donation is turned off, the VDD charge rearrangement for NO^+ is only slightly reduced to $\Delta Q = -0.839$ e, whereas turning-off π-backdonation causes NO^+ to adopt a positive charge of $\Delta Q = +0.022$ e.

In this way, concerning the ΔE_{int} between the two fragments, if σ-donation is cancelled, we still have an attractive interaction by -4.8 kcal mol^{-1}. However, this is not the case if π-backdonation is suppressed, as we would get a dramatically repulsive interaction that amounts to $+133.9$ kcal mol^{-1}. Thus, π-backdonation is not only larger than the σ-donation Ru–NO bonding mechanism, but it is crucial to have an attractive interaction between $[RuCl(NH_3)_4]^+$ and NO^+ fragments in this *trans*-$[RuCl(NO)(NH_3)_4]^{2+}$ complex. We conclude that the σ–π synergism is necessary in order to yield a stabilizing Ru–NO bond in *trans*-$[RuCl(NO)(NH_3)_4]^{2+}$.

2.4. Chloride *trans* Influence

Next, we investigate how and why the *trans* ligand Cl^- affects the Ru–NO bond. To this end, we first analyze this bond in the absence of the chloride ligand, that is, we investigate the interaction between $[Ru(NH_3)_4]^{2+}$ and NO^+ in $[Ru(NO)(NH_3)_4]^{3+}$ at the same geometry of the *trans*-$[RuCl(NO)(NH_3)_4]^{2+}$ complex. In $[Ru(NO)(NH_3)_4]^{3+}$, at variance with *trans*-$[RuCl(NO)(NH_3)_4]^{2+}$, the Ru–NO interaction energy ΔE_{int} (51.2 kcal mol^{-1}) is clearly repulsive (see II in Table 2). This net repulsive character mainly originates from the large electrostatic repulsion between the two positively charged fragments ($\Delta V_{elstat} = 171.7$ kcal mol^{-1}) that, together with ΔE_{Pauli} (79.3 kcal mol^{-1}), overrule the attractive ΔE_{oi} (-199.8 kcal mol^{-1}).

The highly repulsive ΔV_{elstat} is attributed to the lack of the negatively charged Cl^- ligand. The absence of the *trans* Cl^- ligand also goes with significant changes in the orbital interactions, as reflected by the ΔE_{oi} term. Thus, if we take away the Cl^- ligand, the σ component becomes more stabilizing (going from -32.5 to -43.0 kcal mol^{-1}), but the π component is considerably weakened (going from -196.3 to -151.9 kcal mol^{-1}). Analysis of the Kohn–Sham orbital interaction mechanism indeed reveals a stronger donor–acceptor mixing between the interacting σ FMOs and a weaker mixing between the π FMOs. This is also reflected by the gross Mulliken populations of the FMOs involved, which show larger σ-donation from NO^+:σ ($P = 1.64$ e) to Ru:d_σ* ($P = 0.37$ e), but smaller π-backdonation from Ru:d_π ($P = 1.53$ e) to NO^+:π* ($P = 0.47$ e) in $[Ru(NO)(NH_3)_4]^{3+}$, as compared to $[RuCl(NO)(NH_3)_4]^{2+}$ (see Table 2). The stronger σ-donation from, and weaker π backdonation to, NO^+ translates into a less negative VDD charge (-0.712 e) of the ligand (see Table 2).

To precisely understand how introducing Cl^- modifies the bonding capability of the ruthenium complex towards NO^+, we undertake a bonding analysis of the Ru–Cl bond between $[Ru(NH_3)_4]^{2+}$ and Cl^- in $[RuCl(NH_3)_4]^+$ (see III in Table 2). In this case, the ΔE_{int} is largely attractive (-257.5 kcal mol^{-1}), especially owing to the very attractive ΔV_{elstat} (-304.7 kcal mol^{-1}) term between the cationic and anionic fragments. The orbital interactions ΔE_{oi} (-92.3 kcal mol^{-1}) arise from the Cl^- ligand σ-donating charge to the [Ru] fragment (see Figure 2), from Cl^-:p_σ ($P = 1.43$ e) to Ru:d_σ* ($P = 0.53$ e). There is no π-backdonation (Ru:d_π $P = 1.97$ e), as Cl^- has no π acceptor orbitals. This is the reason why σ orbital interactions are larger than π. As a consequence, the Cl^- ligand loses $\Delta Q = 0.226$ electrons, which are transferred to the [Ru] fragment (see Table 2). Importantly, the Cl–Ru orbital interactions push the Ru d_π orbitals up in energy in a Pauli repulsive Cl^-:3p_π-[Ru]:d_π closed-shell interaction (see Figure 2). This is the main responsible mechanism that enhances the π-backdonation capability of the resulting $[RuCl(NH_3)_4]^+$ fragment towards NO^+. In line with this mechanism, a *trans* F^- ligand reinforces the Ru–NO^+ coordination bond even more than *trans* Cl^-, because of a stronger F^-:2p_π-[Ru]:d_π closed-shell interaction (not shown in Figure 2). Thus, going from *trans*-$[Ru\mathbf{Cl}(NO)(NH_3)_4]^{2+}$ to *trans*-$[Ru\mathbf{F}(NO)(NH_3)_4]^{2+}$, π-backbonding interactions are enhanced. Accordingly, the net transfer of charge to the NO^+ ligand increases from 0.892 to 0.904 e, the Ru–NO^+ bond energy ΔE strengthens from -56.6 to -68.9 kcal mol^{-1}, and the bond shortens from 1.838 to 1.766 Å (data for *trans*-F^- case not shown).

We conclude that the *trans* Cl^- ligand reinforces the Ru–NO bond in *trans*-$[RuCl(NO)(NH_3)_4]^{2+}$ by reducing the electrostatic repulsion as well as by strengthening the π-backdonation.

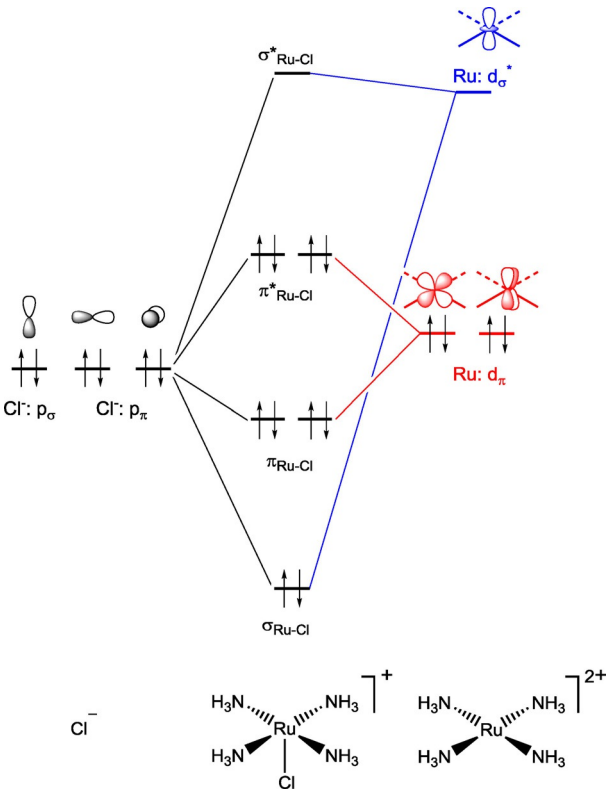

Figure 2. Orbital interaction diagram with the processes of σ-donation (blue) and π-backdonation (red) of Ru–NO present in $[RuCl(NH_3)_4]^+$ composed of Cl^- and $[Ru(NH_3)_4]^{2+}$, emerging from our Kohn–Sham orbital analyses at ZORA-BP86/TZ2P.

2.5. Ru–CO Interaction

To demonstrate that our findings are applicable more generally, we have substituted NO^+ for the isoelectronic CO in the equivalent *trans*-$[RuCl(CO)(NH_3)_4]^+$ complex. In the case of the CO ligand, there is no discussion about the canonical form. The interaction between $[RuCl(NH_3)_4]^+$ and CO has been analyzed by means of an EDA (see Table 2). One might expect that the Ru–CO bond is much stronger than the Ru–NO bond, because the latter occurs between two fragments of the same charge, whereas the former does not. Strikingly, however, Ru–CO ($\Delta E_{int} = -69.2$ kcal mol^{-1}) is only 4.6 kcal mol^{-1} stronger than the Ru–NO bond ($\Delta E_{int} = -64.6$ kcal mol^{-1}).

Indeed, the ΔV_{elstat} term goes from repulsive in *trans*-$[RuCl(NO)(NH_3)_4]^{2+}$ ($+55.2$ kcal mol^{-1}) to very attractive in *trans*-$[RuCl(CO)(NH_3)_4]^+$ (-136.8 kcal mol^{-1}). However, Pauli repulsion increases to 192.4 kcal mol^{-1}, and ΔE_{oi} weakens to only -124.8 kcal mol^{-1}. The weakening in the orbital interaction terms from Ru–NO^+ to Ru–CO results from a significant weakening in π-backbonding to the neutral CO, which dominates the strengthening in σ donation. These trends also show up in the FMO mixing patterns, as reflected by the FMO population of Ru:d_π ($P = 1.73$ e.).

Thus, despite the similar interaction energy between Ru and either NO or CO ligands in the complexes under analysis, their bonding character is rather different. Ru–NO is bonded thanks to a very attractive covalent π component, even though the interaction is electrostatically repulsive. On the other hand, the Ru–CO interaction is characterized by a more balanced attractive electrostatic and covalent σ and π components.

3. Conclusions

The *trans*-$[RuCl(NO)(NH_3)_4]^{2+}$ complex is best conceived as consisting of $[RuCl(NH_3)_4]^+$ and the nitrosyl cation NO^+ held together by a Ru^{II}–NO^+ coordination bond. This follows from our relativistic density functional theory computations, which show that: i) this is the energetically by far preferred dissociation mode; ii) the Cl–Ru–NO angle is 180°; and iii) the Kohn–Sham molecular orbital electronic structure of the complex arises from $Ru^{II} \leftarrow NO^+$ σ-donation and $Ru^{II} \rightarrow NO^+$ π-backdonation.

Our quantitative bonding analyses show that there is synergy between σ-donation and π-backdonation, and that the latter is the dominant term in the Ru^{II}–NO^+ coordination bond. Interestingly, the electrostatic interaction across Ru^{II}–NO^+ is pronouncedly repulsive, owing the Coulomb repulsion between the two singly positively charged fragments of $[RuCl(NH_3)_4]^+$ and NO^+ that are formed in the lowest-energy dissociation mode. It is the synergistic orbital interactions that compensate for both the electrostatic repulsion as well as the Pauli repulsion between closed shells, and thus keep this bond together.

Finally, we have identified, in detail, the mechanism behind the negative *trans* influence of the Cl^- ligand. This ligand, which is oriented *trans* with respect to the NO^+ ligand, reinforces the Ru^{II}–NO^+ bond in two ways: i) it reduces the electrostatic repulsion by reducing the negative charge of the ruthenium fragment and ii) it strengthens π-backdonation by pushing up the ruthenium d_π orbitals.

Acknowledgements

We thank São Paulo Research Foundation (FAPESP) (grants 2008/02677-0, 2011/20351-7, 2014/50265-3 and 2015/15176-2), CNPq (grants 481560/2010-6 and 304393/2013-4), CAPES (process 1938-14), The Netherlands Organization for Scientific Research (NWO-CW and NWO-EW), and Spanish MINECO (project CTQ2016-77558-R) for financial support.

Conflict of Interest

The authors declare no conflict of interest.

Keywords: molecular orbital analysis · negative *trans* influence · nitric oxide · ruthenium complexes · synergy

[1] a) L. J. Ignarro in *Nitric Oxide: Biology and Pathobiology, 2nd ed.*, Academic Press, **2010**; Burlington (USA); b) D. A. Wink, J. B. Mitchell, *Free Radicals Biol. Med.* **1998**, *25*, 434–456; c) P. Pacher, J. S. Beckman, L. Liaudet, *Physiol. Rev.* **2007**, *87*, 315–424; d) E. Karpuzoglu, S. A. Ahmed, *Nitric Oxide* **2006**, *15*, 177–186; e) N. N. Finer, K. J. Barrington, *Cochrane Database of Systematic Reviews*, **2006**, https://doi.org/10.1002/14651858.CD000399.pub2; f) J. C. Toledo, Jr., A. Ohara, *Chem. Res. Toxicol.* **2012**, *25*, 975–989.

[2] a) P. C. Ford, I. M. Lorkovic, *Chem. Rev.* **2002**, *102*, 993–1018; b) R. L. Klimish, J. G. Larson, *The Catalytic Chemistry of Nitrogen Oxides*, Plenum, New York, **1975**; c) K. K. Pandey, *Coord. Chem. Rev.* **1983**, *51*, 69–98; d) G. B. Richter-Addo, P. Legzdins, *Metal Nitrosyls*, Oxford University Press, New York, **1992**, and references therein; e) C. S. Allardyce, P. J. Dyson, *Platinum Met. Rev.* **2001**, *45*, 62–69; f) F. Bottomley, *Coord. Chem. Rev.* **1978**, *26*, 7–32; g) F. G. Doro, I. M. Pepe, S. E. Galembeck, R. M. Carlos, Z. N. da Rocha, M. Bertotti, E. Tfouni, *Dalton Trans.* **2011**, *40*, 6420–6432; h) E. Tfouni, M. Krieger, B. R. McGarvey, D. W. Franco, *Coord. Chem. Rev.* **2003**, *236*, 57–69; i) F. G. Doro, K. Q. Ferreira, Z. N. da Rocha, G. F. Caramori, A. J. Gomes, E. Tfouni, *Coord. Chem. Rev.* **2016**, *306*, 652–677.

[3] a) J. B. Coe, J. S. Glenwright, *Coord. Chem. Rev.* **2000**, *203*, 5–80; b) J. H. Enemark, R. D. Feltham, *Coord. Chem. Rev.* **1974**, *13*, 339–406; c) K. C. Jørgensen, *Coord. Chem. Rev.* **1966**, *1*, 164–178; d) A. Franke, F. Roncaroli, R. van Eldik, *Eur. J. Inorg. Chem.* **2007**, 773–798; e) T. A. Albright, J. K. Burdett, M. H. Whangbo, *Orbital-Interactions in Chemistry*, Wiley, New York, **1985**; f) G. F. Caramori, A. G. Kunitz, K. F. Andriani, F. G. Doro, G. Frenking, E. Tfouni, *Dalton Trans.* **2012**, *41*, 7327–7339.

[4] C. Fonseca Guerra, J.-W. Handgraaf, E. J. Baerends, F. M. Bickelhaupt, *J. Comput. Chem.* **2004**, *25*, 189–210.

[5] G. te Velde, F. M. Bickelhaupt, E. J. Baerends, C. Fonseca Guerra, S. J. A. van Gisbergen, J. G. Snijders, T. Ziegler, *J. Comput. Chem.* **2001**, *22*, 931–967.

[6] E. van Lenthe, E. J. Baerends, *J. Comput. Chem.* **2003**, *24*, 1142–1156.

[7] C. Fonseca Guerra, O. Visser, J. G. Snijders, G. te Velde, E. J. Baerends, *Methods and Techniques for Computational Chemistry*, STEF, Cagliari, **1995**, and references therein.

[8] J. C. Slater, *Phys. Rev.* **1951**, *81*, 385–390.

[9] S. H. Vosko, L. Wilk, M. Nusair, *Can. J. Phys.* **1980**, *58*, 1200–1211.

[10] J. P. Perdew, *Phys. Rev. B* **1986**, *33*, 8822–8824. Erratum: J. P. Perdew, *Phys. Rev. B* **1986**, *33*, 7406.

[11] A. D. Becke, *Phys. Rev. A* **1988**, *38*, 3098–3100.

[12] E. van Lenthe, E. J. Baerends, J. G. Snijders, *J. Chem. Phys.* **1993**, *99*, 4597–4610.

[13] a) F. M. Bickelhaupt, E. J. Baerends, In: *Reviews in Computational Chemistry*; (Eds. K. B. Lipkowitz, D. B. Boyd.); Wiley-VCH, New York, **2000**, Vol.

15, pp. 1–86; b) T. Ziegler, A. Rauk, *Theor. Chim. Acta* **1977**, *46*, 1–10; c) T. Ziegler, A. Rauk, *Inorg. Chem.* **1979**, *18*, 1558–1565; d) T. Ziegler, A. Rauk, *Inorg. Chem.* **1979**, *18*, 1755–1759.

[14] F. M. Bickelhaupt, N. J. R. van Eikema Hommes, C. Fonseca Guerra, E. J. Baerends, *Organometallics* **1996**, *15*, 2923–2931.

[15] a) C. F. Guerra, F. M. Bickelhaupt, J. G. Snijders, E. J. Baerends, *Chem. Eur. J.* **1999**, *5*, 3581–3594; b) C. Kittel, *Introduction to Solid State Physics*, Wiley, New York, **1986**.

[16] G. te Velde, E. J. Baerends, *J. Comput. Phys.* **1992**, *99*, 84–98.

[17] a) M. A. Il'in, V. A. Emel'yanov, I. A. Baidina, N. I. Alferova, I. V. Korol'kov, *Zh. Neorg. Khim.* **2007**, *52*, 67–75; b) J. C. Toledo, Jr., H. A. S. Silva, M. Scarpellini, V. Mori, A. J. Camargo, M. Bertotti, D. W. Franco, *Eur. J. Inorg. Chem.* **2004**, 1879–1885; c) C. W. B. Bezerra, S. C. da Silva, M. T. P. Gambardella, R. H. A. Santos, L. M. A. Plicas, E. Tfouni, D. W. Franco, *Inorg. Chem.* **1999**, *38*, 5660–5667.

Received: February 8, 2017
Version of record online March 30, 2017

